Interfacial layer formation and thermal transport mechanisms in polymer nanocomposites for vibration-damping applications

Alexander Antonov[1], Khurshidbek Nurmetov[2], Alimjon Riskulov[3], Vasily Struk[4], Alexander Nikitin[5], Ziarat Pashayeva[6]
[1, 4]Department of Materials Science and Resource-Saving Technologies, Yanka Kupala State University of Grodno, Grodno, Belarus
[2, 3]Department of Materials Science and Mechanical Engineering, Tashkent State Transport University, Tashkent, Uzbekistan
[5]Department of Theoretical Physics and Thermal Engineering, Yanka Kupala State University of Grodno, Grodno, Belarus
[6]Institute of Petrochemical Processes, Ministry of Science and Education of Azerbaijan, Baku, Azerbaijan
[6]Azerbaijan State Oil and Industry University, Baku, Azerbaijan
[2]Corresponding author
E-mail: [1]*antonov.science@gmail.com*, [2]*behbudbek@gmail.com*, [3]*olimjonr2008@mail.ru*, [4]*struk@grsu.by*, [5]*nik@grsu.by*, [6]*ziyaretchem@gmail.com*

Received 4 March 2026; accepted 19 April 2026; published online 8 June 2026
DOI https://doi.org/10.21595/vp.2026.26270

Check for updates

76th International Conference on Vibroengineering in Tashkent, Uzbekistan, April 28-29, 2026

Abstract. This study investigates the mechanisms of interfacial layer formation in polymer nanocomposites and their influence on thermal transport properties. Experimental evaluation of epoxy composites modified with Al_2O_3 and SiO_2 particles of varying dispersity demonstrates that reduced modifier size leads to increased effective thermal conductivity, attributed to the formation of three-dimensional physical bond networks between matrix and nanoparticles. A finite-difference numerical model incorporating interfacial thermal resistance (Kapitza resistance) was developed to calculate temperature fields and effective thermal conductivity. Model validation against experimental data yields interfacial layer thicknesses of 6.75 nm for Al_2O_3-filled composites at 0.312 volume fraction. The structuring influence of nanoscale modifiers promotes formation of physical and chemical bonds at the interface, enhancing thermal conductivity of the boundary layer. These mechanisms enable targeted control of polymer nanocomposite properties for vibration-damping components requiring simultaneous thermal management and mechanical energy dissipation in automotive and mechanical engineering applications.

Keywords: polymer nanocomposites, interfacial layer, thermal conductivity, Kapitza resistance, finite-difference modeling, vibration damping, energy dissipation.

1. Introduction

Polymer nanocomposites based on high-molecular-weight matrices are increasingly employed in mechanical engineering for functional elements of machines, mechanisms, and technological equipment requiring controlled energy dissipation [1-6]. However, understanding the mechanisms of nanocomposite structure formation presents challenges associated with ambiguity in dimensional parameters and identification of determining factors governing nanoparticle influence on matrix structural evolution [7-9].

The ideal structure of a nanocomposite material comprises three components: the matrix component (M), dispersed particle (P), and boundary layer (L) (Fig. 1). The boundary layer – a region of modified matrix surrounding each nanoparticle – critically determines macroscopic properties including mechanical damping and thermal transport.

Thermal management has emerged as a critical consideration in vibration-damping applications, as mechanical energy dissipation generates heat that must be efficiently conducted

away from the damping element. Polymers traditionally used as matrices exhibit thermal conductivity coefficients of 0.1-0.5 W/m·K. Even fillers with high intrinsic thermal conductivity (e.g., carbon nanotubes at 3000 W/m·K) do not alone solve this problem, as interfacial thermal resistance (Kapitza resistance) dominates the composite's effective thermal conductivity [10], [11]. Furthermore, as particle size approaches the nanoscale, the intrinsic thermal conductivity of the filler itself can decrease due to phonon boundary scattering, a factor often overlooked in classical effective medium theories [12], [13].

This study addresses the fundamental mechanisms of interfacial layer formation and their influence on thermal transport by proposing a numerical method for calculating the effective thermal conductivity of filled polymer systems. The essence of the proposed method lies in the direct solution of the heat conduction equation using finite-difference techniques, with careful consideration of the relevant boundary and initial conditions. The model uniquely accounts for the structural distribution of filler particles and introduces an intermediate boundary layer to quantitatively describe matrix-filler interactions. For validation, the numerical results are compared against experimental data for epoxy composites filled with Al_2O_3 and SiO_2 nanoparticles, as reported by Kochetov et al. [11]. While many studies focus on either the mechanical damping or thermal conductivity of polymer composites [14-19], our work provides a coupled numerical analysis of how interfacial layer formation influences thermal transport specifically in the context of vibration-damping applications. By demonstrating that reduced modifier particle size leads to the formation of three-dimensional physical bond networks, and by back-calculating the characteristic thickness (≈ 6.75 nm) of the thermally modified interphase layer, this study establishes quantitative structure-property relationships that enable the rational design of polymer nanocomposites for integrated vibration-damping and thermal management applications in automotive and mechanical engineering.

2. Materials and methods

2.1. Experimental foundation and model validation data

The polymer matrix employed was epoxy resin (ER) (ED-20 grade, epoxy number 20.1-22.5, GOST 10587-84) cured with polyethylenepolyamine (10 parts per hundred resin). Modifiers included:

1) Al_2O_3: α-phase, particle size ranges: ≈ 30 nm.

2) SiO_2: amorphous, particle size ranges: ≈ 20 nm.

For the validation of the proposed numerical model, we utilized the experimental data on the effective thermal conductivity of these specific epoxy-based nanocomposites as reported by Kochetov et al. [11]. In the referenced study, the composites were fabricated using surface-modified nanoparticles to ensure homogeneous dispersion within the epoxy matrix via shear mixing and ultrasonication, followed by curing. This dataset was selected as a reliable benchmark due to the detailed characterization of both filler volume fraction and thermal response.

3. Numerical method and finite-difference scheme

To calculate the effective thermal conductivity, we propose a direct numerical solution of the three-dimensional steady-state heat conduction equation. The essence of the method lies in explicitly accounting for the structural distribution of filler particles and introducing an intermediate boundary layer to describe the matrix-filler thermal interaction (Kapitza resistance).

The differential heat conduction equation is as Eq. (1):

$$\frac{\partial}{\partial x}\left(\lambda_x \frac{\partial T}{\partial x}\right) + \frac{\partial}{\partial y}\left(\lambda_y \frac{\partial T}{\partial y}\right) + \frac{\partial}{\partial z}\left(\lambda_z \frac{\partial T}{\partial z}\right) = 0. \quad (1)$$

Boundary conditions:

– $T = T_b$, $x = 0$, $L \geq y \geq 0$, $L \geq z \geq 0$; Dirichlet boundary conditions.

– $T = T_e$, $x = L$, $L \geq y \geq 0$, $L \geq z \geq 0$; Dirichlet boundary conditions.

The problem is solved using a finite-difference scheme (cross scheme) as illustrated in Fig. 2. The discretized equation for the temperature at a node (i, j, k) is expressed in terms of its neighbors. The thermal resistance between the matrix and filler nodes is given by R_δ (Kapitza resistance).

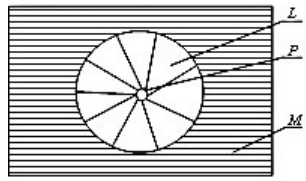

Fig. 1. Schematic representation of nanocomposite material structure: M – matrix, P – particle, L – boundary layer

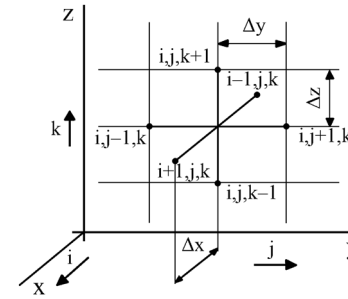

Fig. 2. Cross scheme for the numerical solution of Eq. (8)

3.1. Iterative calibration of interfacial resistance

The numerical model contains one unknown parameter: the interfacial thermal resistance R_δ. The modeling strategy consists of:

1) Generating a representative volume element (RVE) with randomly distributed filler particles at a given volume fraction C_V.

2) Assigning bulk thermal conductivity values to the matrix (λ_m) and filler (λ_f).

3) Assigning a trial value to R_δ.

4) Computing λ_{eff} using the finite-difference solver.

5) Comparing the calculated λ_{eff} with the experimental value λ_{exp} from [11] for the same filler content.

6) Iteratively adjusting R_δ until convergence is achieved ($\lambda_{eff} \approx \lambda_{exp}$).

4. Results and discussion

Based on general considerations, the volume concentration of the nanofiller, C_V, is determined from Eq. (2):

$$C_V = \left(1 + \frac{m_M}{m_B} - \frac{\rho_M}{\rho_B}\right)^{-1}, \tag{2}$$

where m_M and m_B are the mass of the modifier particles and the binder, respectively; ρ_M and ρ_B are the specific gravity of the modifier and the binder.

For a modified (interfacial) layer thickness h, Eq. (3) must be satisfied to achieve the maximum modifying effect:

$$4/3\pi(r + h)^3 \cdot n \cdot K = 1, \tag{3}$$

where K is a coefficient accounting for the overlap and compactness of the modified interfacial layer, r is the modifier particle radius, and n is the number of particles. Considering that $m_M \gg m_B$, Eq. (3) can be presented in the form Eq. (4):

$$\frac{h}{r} = \left(\frac{\rho_M}{\rho_B \cdot C_B \cdot K}\right)^{1/3}. \quad (4)$$

It follows from this expression that for the case of a uniform distribution of modifier particles, where they are located at points corresponding to the densest packing of spheres with a radius of $r + h$, and where there is no overlap of the modified regions, the coefficient $K = 0.74$. For a typical ratio of $\rho_M/\rho_B = 4$ and a modifier content of 0.1 %, we obtain $h \approx 15r$.

The formation of a transitional (interfacial) layer in the nanocomposite material leads to changes in the parameters of its characteristics due to the formation of physical and chemical bonds. This conclusion is supported by model studies of the thermal conductivity parameters of composites based on epoxy resin modified with Al_2O_3 and SiO_2 of varying dispersity [11].

Polymers traditionally used as matrices have a thermal conductivity coefficient ranging from 0.1 to 0.5 W/m·K. The thermal conductivity coefficient of fillers does not exceed 50 W/m·K. Even the use of carbon nanotubes as a filler, with a specific thermal conductivity coefficient on the order of 3000 W/m·K, does not solve this problem. The filler can alter the structure of the matrix (modification), increasing the region occupied by crystallites compared to the amorphous phase. A comparison of the thermal conductivity of ordered structures and the amorphous polymer phase does not lead to the required increase in the composite's effective thermal conductivity. Thus, the problem of enhancing the thermal conductivity of polymer matrices cannot be solved solely by selecting a filler with high intrinsic thermal conductivity or by modifying the matrix with an inert filler. Important factors are the filler particle distribution structure and size, the interfacial thermal resistance at the "matrix-filler" boundary, and the thermal contact resistance at the "particle-particle" interface, which are determined by the structural features of the interfacial layer.

As evidenced by experimental data, the thermal conductivity of composite materials at filler concentrations below 0.05 % has a negligible effect on the effective thermal conductivity of the polymer matrix, which in this case is an epoxy resin. This is apparently due to the fact that the introduction of an inert filler at such low loadings does not result in a significant influence from the interphase layer on the overall effective thermal conductivity. As the modifier content increases, a divergence emerges in the thermal conductivity trends for composites with different fillers. This discrepancy is attributed to the different intrinsic thermal conductivity values of the selected fillers and, possibly, to the manifestation of interfacial thermal resistance (Kapitza resistance).

Let us consider the methods for estimating the thickness of the interphase layer. A schematic of the interphase region structure is presented in Fig. 3.

Thermal resistance between points 1 and 2 is determined from Eq. (5):

$$R = \frac{\Delta x}{2\lambda_1} + \frac{\Delta x}{2\lambda_2} + R_\delta. \quad (5)$$

The heat balance Eq. (6):

$$\frac{\lambda_{eff}}{\Delta x}(T_2 - T_1) = \frac{(T_2 - T_1)}{\frac{\Delta x}{2\lambda_1} + \frac{\Delta x}{2\lambda_2} + R_\delta}. \quad (6)$$

Hence:

$$\lambda_{eff} = \frac{1}{\frac{\Delta x}{2\lambda_1} + \frac{\Delta x}{2\lambda_2} + \frac{R_\delta}{\Delta x}}. \quad (7)$$

By varying R_δ, we achieve equality between λ_{eff} and λ_{exp}. As a result, we obtain the value

of Rδ that corresponds to the experimental data. Subsequently, we can calculate the thickness of the interphase layer Eq. (8):

$$\delta = \lambda_{eff} R_{\delta}. \tag{8}$$

Fig. 4 presents the theoretical and experimental curves of the thermal conductivity coefficient as a function of filler content. By varying the parameter of thermal interfacial resistance, we achieve a match between the theoretical and experimental dependencies.

According to experimental data for the composite with Al_2O_3 filler at a concentration of 0.312, the effective thermal conductivity is 0.675 W/m·K. Using software [11], we calculated the effective thermal conductivity of the composite under corresponding conditions for different values of thermal interfacial resistance until the calculated value matched the experimental value for the effective thermal conductivity. In our case, this result was achieved at a thermal resistance of 1×10^{-8} m^2·K/W. Then, using Eq. (8), we calculated the thickness of the thermal interphase layer, which was 6.75 nm [10].

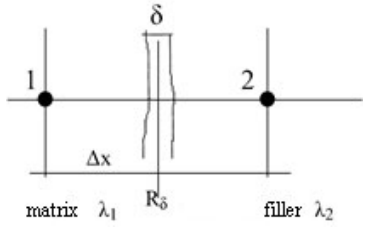

Fig. 3. Interfacial region schematic

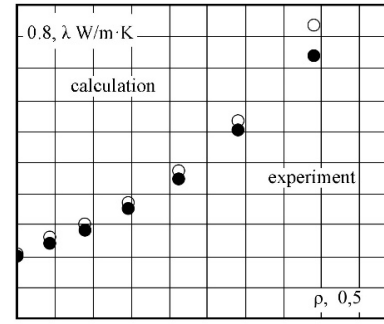

Fig. 4. Implementation of the interfacial layer thickness evaluation method for an Al_2O_3-filled composite

The successful calibration of the model yields $R_{\delta} = 1\times10^{-8}$ m^2·K/W and an interphase layer thickness of $\delta = 6.75$ nm. To further validate the physical relevance of this parameter and to address the underlying mechanisms of thermal transport in these nanocomposites, we conducted an analysis of the size-dependent intrinsic thermal conductivity of the filler particles.

The thermal transport in nanoscale fillers differs significantly from their bulk counterparts. The reduction in particle size leads to increased phonon boundary scattering, which can be quantified by the Knudsen number $K_n = l/L$, where l is the phonon mean free path and L is the characteristic particle size. Using the Debye model and kinetic theory (Table 1), we estimated the thermal conductivity of various ceramic particles as a function of size.

Table 1. Parameters for Evaluating size-dependent thermal conductivity of fillers

Material	Debye temperature θ_D, K	Bulk λ, W/m·K	Phonon MFP l, nm	L_0, nm
Al_2O_3	1030-1050	30-35	5.0	7.13
SiO_2	400-600	~1.38	0.5	10.28
*Note: L_0 is the critical size boundary for nano-state behavior calculated as $L_0 = 230 \cdot \theta_D^{-1/2}$ [nm] [20]				

As is known, the effective thermal conductivity of a composite is associated with a large number of factors: filler concentration, thermal conductivity of the matrix, thermal conductivity of the filler, degree of modification, filler clustering, interfacial thermal resistance, and thermal contact resistance between filler particles [15], [17], [20].

Based on these considerations, we estimated the thermal conductivity coefficient of an epoxy composite with filler particle sizes of $d > 500$ nm.

The heat flow method involves calculating the composite's temperature field and determining

the heat flux, which is used to calculate the effective thermal conductivity of the composite.

The differential heat conduction equation is as Eq. (1). The problem is solved using a finite-difference scheme (for the stationary case) according to the diagram shown in Fig. 2.

The equation (in finite differences for the non-stationary case) is given by Eq. (9):

$$\begin{aligned}&\frac{\lambda_{ijk}^{(x)}-\lambda_{(i-1)jk}^{(x)}}{\Delta x}\times\frac{T_{ijk}-T_{(i-1)jk}}{\Delta x}+\lambda_{ijk}^{(x)}\frac{T_{(i-1)jk}-2T_{ijk}+T_{(i+1)jk}}{\Delta x^2}\\&+\frac{\lambda_{ijk}^{(y)}-\lambda_{i(j-1)k}^{(y)}}{\Delta y}\times\frac{T_{ijk}-T_{i(j-1)k}}{\Delta y}+\lambda_{ijk}^{(y)}\frac{T_{i(j-1)k}-2T_{ijk}+T_{i(j+1)k}}{\Delta y^2}\\&+\frac{\lambda_{ijk}^{(z)}-\lambda_{ij(k-1)}^{(z)}}{\Delta z}\times\frac{T_{ijk}-T_{ij(k-1)}}{\Delta z}+\lambda_{ijk}^{(z)}\frac{T_{ij(k-1)}-2T_{ijk}+T_{ij(k+1)}}{\Delta z^2}\\&=\rho_{ijk}c_{ijk}\frac{T_{ijk,l}-T_{ijk,l-1}}{\Delta t},\end{aligned}\tag{9}$$

where T_{ijk} is the temperature at the grid nodes; $\lambda_{ijk}^{(x,y,z)}$ is the thermal conductivity coefficient; Δx, Δy, Δz are the grid periods; Δt is the time step; $\rho_{ijk}c_{ijk}$ is the density and heat capacity of the material.

Transforming Eq. (9) for the non-stationary case for the temperature field yields the model. The temperature of a node can be expressed through the temperatures of the adjacent nodes:

$$\begin{aligned}T_{ijk,l}&=\frac{\Delta t}{\rho_{ijk}c_{ijk}}(A_1+A_2+A_3)+T_{ijk},\\A_1&=\frac{\lambda_{ijk}^{(x)}-\lambda_{(i-1)jk}^{(x)}}{\Delta x}\times\frac{T_{ijk}-T_{(i-1)jk}}{\Delta x}+\lambda_{ijk}^{(x)}\frac{T_{(i-1)jk}-2T_{ijk}+T_{(i+1)jk}}{\Delta x^2},\\A_2&=\frac{\lambda_{ijk}^{(y)}-\lambda_{i(j-1)k}^{(y)}}{\Delta y}\times\frac{T_{ijk}-T_{i(j-1)k}}{\Delta y}+\lambda_{ijk}^{(y)}\frac{T_{i(j-1)k}-2T_{ijk}+T_{i(j+1)k}}{\Delta y^2},\\A_3&=\frac{\lambda_{ijk}^{(z)}-\lambda_{ij(k-1)}^{(z)}}{\Delta z}\times\frac{T_{ijk}-T_{ij(k-1)}}{\Delta z}+\lambda_{ijk}^{(z)}\frac{T_{ij(k-1)}-2T_{ijk}+T_{ij(k+1)}}{\Delta z^2}.\end{aligned}\tag{10}$$

For the numerical solution to be stable, the following condition must be satisfied Eq. (11):

$$F_O=\frac{\Delta t\lambda_{ijk}^{(x)}}{\rho_{ijk}c_{ijk}\Delta x^2}<0.5.\tag{11}$$

In the stationary case, the temperature field is determined by the relations Eq. (12):

$$\begin{aligned}T_{ijk}&=\frac{A_2+A_3}{A_1},\\A_1&=\left(\frac{\lambda_{ijk}^{(x)}+\lambda_{(i-1)jk}^{(x)}}{\Delta x^2}+\frac{\lambda_{ijk}^{(y)}+\lambda_{i(j-1)k}^{(y)}}{\Delta y^2}+\frac{\lambda_{ijk}^{(z)}+\lambda_{ij(k-1)}^{(z)}}{\Delta z^2}\right),\\A_2&=\lambda_{(i-1)jk}^{(x)}\frac{T_{(i-1)jk}}{\Delta x^2}+\lambda_{i(j-1)k}^{(y)}\frac{T_{i(j-1)k}}{\Delta y^2}+\lambda_{ij(k-1)}^{(z)}\frac{T_{ij(k-1)}}{\Delta z^2},\\A_3&=\lambda_{ijk}^{(x)}\frac{T_{(i+1)jk}}{\Delta x^2}+\lambda_{ijk}^{(y)}\frac{T_{i(j+1)k}}{\Delta y^2}+\lambda_{ijk}^{(z)}\frac{T_{ij(k+1)}}{\Delta z^2}.\end{aligned}\tag{12}$$

After calculating the temperature at the grid nodes, the average heat flux value at each node is calculated, followed by the effective thermal conductivity coefficient:

$$\lambda_{eff} = L\frac{\sum_1^N \lambda^{(i)}\frac{\partial T}{\partial y}}{T_b - T_e}. \tag{13}$$

Let us present another model for the composite's thermal conductivity. This is the earliest model, proposed by Maxwell Eq. (14):

$$\lambda_{eff} = \lambda_1\left(\frac{\lambda_2 + 2\lambda_1 - 2\rho_2(\lambda_1 - \lambda_2)}{\lambda_2 + 2\lambda_1 + \rho_2(\lambda_1 - \lambda_2)}\right), \tag{14}$$

where λ_1 is the thermal conductivity of the matrix; λ_2 is the thermal conductivity of the filler.

Figs. 5 and 6 present the experimental and calculated data on the effective thermal conductivity of a model composite based on epoxy resin with SiO_2 and Al_2O_3 modifiers of different dispersity.

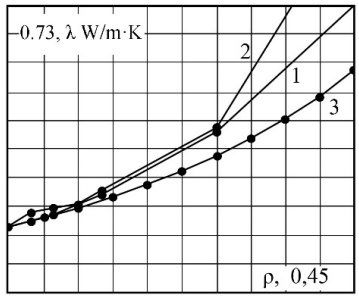

Fig. 5. Dependence of the effective thermal conductivity of an Epoxy/SiO_2 model composite on filler particle size ($d > 200$ nm)
1 – experimental data; 2 – theoretical calculation;
3 – Maxwell model calculation

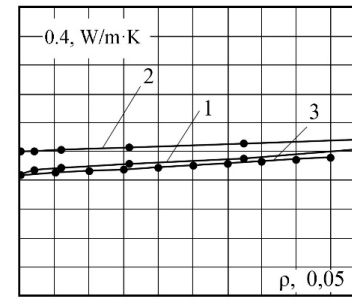

Fig. 6. Effective thermal conductivity of the model epoxy resin + Al_2O_3 composite versus filler particle size (d > 500 nm): 1 – experimental data;
2 – theoretical calculation;
3 – Maxwell model calculation

As shown in the Table 1, the effective thermal conductivity of the filler particle deviates from the bulk value when the particle diameter approaches the phonon mean free path. For Al_2O_3 particles with $d \approx 30$ nm, the intrinsic conductivity is notably lower than the bulk value (30-35 W/m·K). This finding is critical: it explains why the simple Maxwell model (Fig. 5, 6) overestimates the composite's λ_{eff} at higher nanofiller loadings. The competing effects of (1) increased interfacial area (Kapitza resistance) and (2) reduced intrinsic filler conductivity due to phonon confinement both act to suppress the overall effective thermal conductivity compared to micro-composite predictions.

This analysis confirms that the numerical model's ability to match experimental data is not merely a curve-fitting exercise, but is physically justified by the interfacial thermal resistance R_δ and the modified transport properties within the nanoscale filler and its boundary layer.

As evidenced by the data, a reduction in the modifier particle size favorably impacts the increase in the effective thermal conductivity coefficient. This effect may be attributed to the structuring action of the modifier particle in its nano-state, which possesses elevated energy parameters that promote the formation of a spatial network of physical bonds between the matrix polymer and the modifier. The formation of such bonds contributes to an increase in the thermal conductivity of the composite's boundary layer [10], [14], [16].

5. Conclusions

This study establishes the fundamental mechanisms of interfacial layer formation in polymer nanocomposites and their influence on thermal transport properties. Numerical estimate confirmed

by experimental data of epoxy composites modified with Al_2O_3 and SiO_2 demonstrates that variation in modifier particle size induces a significant change in the effective thermal conductivity of the composite. This behavior is primarily attributed to the size-dependent modification of the intrinsic thermophysical properties of the filler particles (such as phonon scattering effects), coupled with the formation of a structured interphase layer characterized by three-dimensional physical bond networks between the matrix and nanoparticles.

The proposed numerical method, which solves the heat conduction equation via finite-difference techniques while incorporating an intermediate boundary layer, has been successfully validated against reference experimental data for Al_2O_3 and SiO_2 nanoparticle-filled epoxy composites [11]. This approach not only accurately predicts effective thermal conductivity but also enables the quantitative estimation of the interfacial layer thickness (e.g., 6.75 nm for Al_2O_3). These findings confirm that the developed model effectively captures the influence of nanofiller dispersity and interfacial interactions on thermal transport, offering a robust tool for engineering polymer nanocomposites with enhanced thermal management capabilities.

These findings have direct applications in automotive and mechanical engineering, where vibration-damping components must efficiently dissipate both mechanical energy (as heat) and the resulting thermal energy. The developed structure-property relationships enable rational design of nanocomposite materials for engine mounts, suspension bushings, and structural damping elements requiring integrated vibration control and thermal management. Targeted control of interfacial layer formation through modifier selection based on the nano-state criterion provides a systematic approach to developing next-generation damping materials with enhanced performance and reliability.

Acknowledgements

The authors have not disclosed any funding.

Data availability

The datasets generated during and/or analyzed during the current study are available from the corresponding author on reasonable request.

Conflict of interest

Prof. Khurshidbek Nurmetov is a scientific committee member of the 76th International Conference on Vibroengineering and was not involved in the editorial review and/or the decision to publish this article.

References

[1] S. V. Avdeychik et al., *Nanocomposite Engineering Materials: Development and Application experience*. Grodno: GrSU, 2006.

[2] S. V. Avdeychik et al., *Polymer-Silicate Engineering Materials: Physical Chemistry, Technology, application*. Grodno: Tekhnalogiya, 2007.

[3] V. A. Struk et al., *Nanomaterials and Nanotechnologies for Mechanical Engineering*. Minsk: RIVSH, 2021.

[4] A. S. Antonov, S. V. Avdeychik, and A. G. Ikromov, *Energy Factor in Materials Science and Technology of Polymer Composites*. Minsk: Vneshinvestprom, 2019.

[5] S. V. Avdeychik, V. A. Struk, and A. S. Antonov, *The Factor of Nano-State in Materials Science of Polymer Nanocomposites*. Saarbrücken: LAP LAMBERT Academic Publishing, 2017.

[6] A. A. Abdurazakov, S. V. Avdeychik, and A. S. Antonov, *Composite Materials in High-Resource Belt Conveyor Structures*. Minsk: Vneshinvestprom, 2019.

[7] A. I. Gusev, *Nanomaterials, Nanostructures, Nanotechnologies*. Moscow: Fizmatlit, 2005.

[8] P. M. Ajayan, L. S. Schalder, and A. V. Braun, *Nanocomposite Science and Technology*. Weinheim: Wiley, 2003, https://doi.org/10.1002/3527602127

[9] C. P. Poole and F. J. Owens, *Nanotechnology*. Moscow: Tekhnosfera, 2005.

[10] A. V. Nikitin and A. V. Belko, "Thermal Kapitsa resistance of the interfacial layer in composite systems with fine disperse filler," *Vesnik of Yanka Kupala State University of Grodno. Series 2*, Vol. 15, No. 1, pp. 137–145, 2025.

[11] R. Kochetov, A. V. Korobko, T. Andritsch, P. H. F. Morshuis, S. J. Picken, and J. J. Smit, "Modelling of the thermal conductivity in polymer nanocomposites and the impact of the interface between filler and matrix," *Journal of Physics D: Applied Physics*, Vol. 44, No. 39, p. 395401, Oct. 2011, https://doi.org/10.1088/0022-3727/44/39/395401

[12] V. I. Khvesyuk and A. S. Skryabin, "Heat conduction in nanostructures," *High Temperature*, Vol. 55, No. 3, pp. 434–456, Jun. 2017, https://doi.org/10.1134/s0018151x17030129

[13] G. Zhang et al., "A percolation model of thermal conductivity for filled polymer composites," *Journal of Composite Materials*, Vol. 44, No. 8, pp. 963–970, 2009, https://doi.org/10.1177/0021998309349690

[14] A. Antonov, K. Nurmetov, A. Riskulov, T. Urazbaev, V. Struk, and D. Nakhvat, "Composite thermoplastic materials for filament production in 3D printing technology," *Vibroengineering Procedia*, Vol. 60, pp. 424–430, Dec. 2025, https://doi.org/10.21595/vp.2025.25691

[15] F. Adilov and S. Makhmudova, "Boundary element method for numerical solution to two-dimensional problems of fracture mechanic," in *AIP Conference Proceedings*, Vol. 3119, No. 1, p. 040001, Jun. 2024, https://doi.org/10.1063/5.0217963

[16] A. Antonov, K. Nurmetov, A. Riskulov, V. Struk, and W. Xuemin, "Composite materials based on polyolefins modified with carbon-containing components," *Vibroengineering Procedia*, Vol. 60, pp. 458–465, Dec. 2025, https://doi.org/10.21595/vp.2025.25690

[17] U. Rakhimov, N. Tursunov, T. Urazbayev, E. Bakhteev, and I. Omonov, "Development of a technology for producing cast iron in an induction crucible furnace, modification in a ladle and casting in a system of casting molds," *Vibroengineering Procedia*, Vol. 60, pp. 416–423, Dec. 2025, https://doi.org/10.21595/vp.2025.25636

[18] S. Absattarov, S. Yunusov, and N. Tursunov, "Research of the stress-strain state and durability of freight wagon trolley springs by the method of finite element modeling in ANSYS," *Vibroengineering Procedia*, Vol. 60, pp. 664–669, Dec. 2025, https://doi.org/10.21595/vp.2025.25532

[19] N. S. Uzdieva, E. M. Bakhteev, K. L. Vakhidova, and S. A. Nazarov, "Improving the quality of cast blanks by applying force to the solidifying metal," *Vibroengineering Procedia*, Vol. 60, pp. 385–392, Dec. 2025, https://doi.org/10.21595/vp.2025.25575

[20] V. A. Liopo, "The size boundary between nano and bulk states: theory and experiment," Vesnik of Yanka Kupala State University of Grodno. Series 2, 2007.